Investigation of solid rocket motor strength characteristics by employing composite materials

A. Fedaravičius*, S. Račkauskas**, E. Sližys***, A. Survila****

*Kaunas University of Technology, Kęstučio 27, 44025 Kaunas, Lithuania, E-mail: algimantas.fedaravicius@ktu.lt
**Kaunas University of Technology, Kęstučio 27, 44025 Kaunas, Lithuania, E-mail: saulius.rackauskas@ktu.lt
***Kaunas University of Technology, Kęstučio 27, 44025 Kaunas, Lithuania, E-mail: egidijus.slizys@ktu.lt
****Kaunas University of Technology, Kęstučio 27, 44025 Kaunas, Lithuania, E-mail: arvydas.survila@ktu.lt

1. Introduction

Products manufactured for the space industry and defence are covered by an exceptional quality control [1]. This used to achieve specific technological processes and production methods. Great attention is given to rocket engines and their parts for their strength characteristics and the reliability of operation setting. The majority of rockets are used to bring cargo into orbit combined with booster systems. Boosters are usually the solid rocket motors which are designed to provide extra lift as additional rocket power for a limited time and provide nominal flight parameters, after depletion they disconnect from the rocket's body and drop into atmosphere for furtherer reuse or just simply burn in atmosphere. After rocket boosters jettisons only the main rocket engine reaches the destination. When lifting cargo into orbit, weight problem is very important. It is also very important to design such systems that the equilibrium of engine mass and its ability would withstand high motor casing stresses, pressures and strains for failure prevention. This way one can save not only space for additional amount of fuel, but with the same amount of fuel raise higher weight loads which would mean lower operating costs per rocket for every mission. To tackle this harness lightweight alloy, engineers employed binders and adhesives. However, the metal structure is characterized by both the electrical conductivity, which is not always possible to use the structure of the relevant components of the engine and on the changes caused by thermal expansion and contraction of metal, thereby compromising the desired tight loose coupling between components or damaging them. Unlike metals – composite materials do not have these properties and are superior in many settings, but unlike the even metal, composite materials are much harder to process into shapes and make ready and working. That technological process is very sophisticated and complex because of quality control which increases the cost of the product. However, despite the fact that composite gains traction in space industry and the current spacecraft without them is unimaginable. The main components made of composite materials are solid rocket motor boosters or fuel tanks to suck liquid fuel such as liquid oxygen (LOX) or liquid hydrogen, etc. The backbone of technological process was employed from textile industry. As the solid fuel rocket motor casing is cylindrical in shape and has unified revolving axis with which fibres can be winded by using the appropriate order structure and desired amount of composite materials. The material itself comes in the form of yarn. A process has been adapted and is widely used in developing rocket motors, boosters and fuel tanks by ESA, NASA and other agencies [2]. The aim of this research is to create finite element model of the solid rocket motor composite casing and to obtain mechanical strength characteristics and ply failure data.

2. Model explanation

The solid rocket motor booster housing is nothing more than a modified pressure vessel so most of the analysis and design techniques can be borrowed from this field of research. Vasiliev describes [3] methods of development for the of composite pressure vessels. In this paper one decides not to use any non-composite linings because of increased product complexity and costs. Usually lining materials are metals or plastics. Specifically in this paper from previous experiments with solid rocket motors was found that maximum pressure in the combustion chamber was almost equal to 6 MPa (Fig. 1) [4]. To explain the model one should note that length of the rocket motor casing is 1006mm, diameter is 160mm, composite thickness is 6mm and it is divided into 3 zones. A – dome, B – cylindrical part, C – nozzle part (Fig. 3).
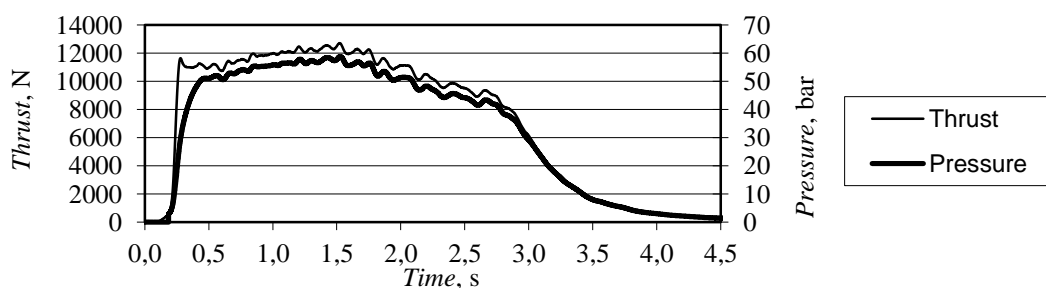

Fig. 1 Graph of rocket motor. Thrust and pressure experimental data

Dome shaped part A is divided into 5 points and one section 6, going from the axis towards the centre of the dome to the equator, which results is measured (Fig. 3). 3 readings are collected: deformation, stress and failures. Cylindrical part B [5] is divided into 3 sections 3, 4, 5 which is also measured in 5 points each. Nozzle part C is divided into 2 sections – converging and diverging 1, 2 which is also measured in 5 points each. Finite element mesh is created separately for different types of components (Fig. 4). The composite element are created using shell type finite element method components. Thermal shield - nozzle part was created as solid part with solid finite element mesh. The simulation is performed using Ansys environment with ACP (Ansys Composite PrePost) plugin [6]. Composite parts model was developed to simulate the carbon fiber wrapping around the prepared mandrel – fuel casing and nozzle parts (on top of them). Model was made from parts of different materials. Composite – carbon fiber and polyester resin [7]. Nozzles thermal protection part was made from machined graphite piece [8]. Below are the mechanical properties of listed materials (Table 1).

Table 1

Mechanical properties of materials

Material table	Density, kg/m^3	Young's modulus, MPa	Shear modulus, MPa
Graphite (TANSO) IG-11	1762	9800	-
Composite-carbon fibre	1490	8600	4700
Polyester resin	1160	3780	1400

Wrapping the corresponding fibre [9] laying down corresponding pattern repeatingly every 3 layers until fulfilment of desired laminate thickness are reached (at this case 12 layers).

- First layer: +45 degrees + resin.
- Second layer: -45 degrees + resin.
- Third layer: close to 90 degrees + resin.

Every single layer is the same thickness like previous one. One layer was described as two-layer composite which is created from filament fiber and resin. The layer thickness is 500 μm. In the following algorithm one provides which inputs and result output has been constructed for the data (Fig 2) [10].
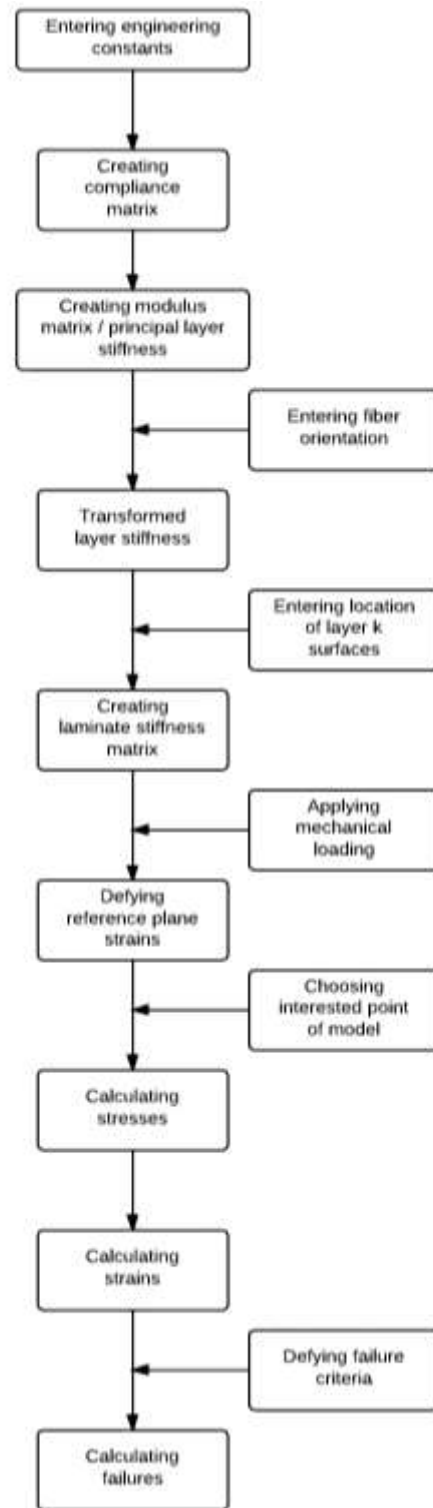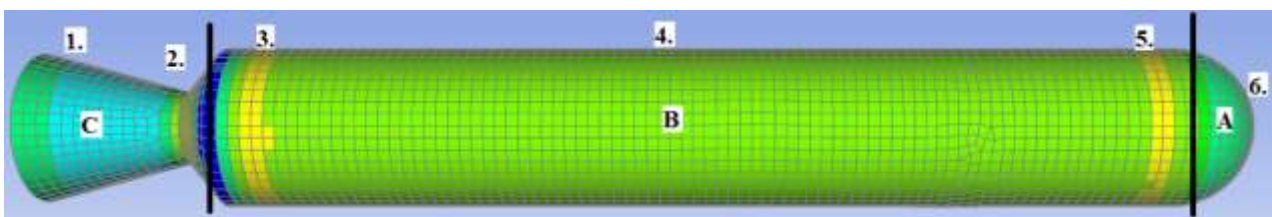
Fig. 2 Algorithm of investigating model
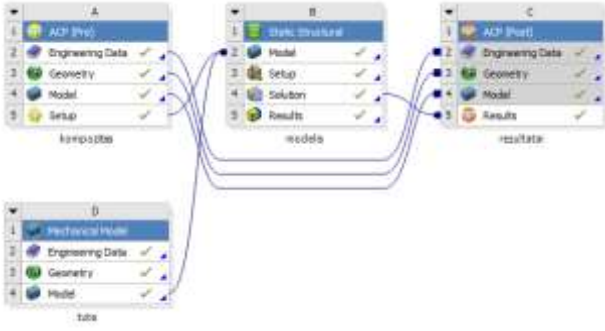
Fig. 3 Probe points

Fig. 4 Chart of used model

3. Mathematical approaches

Longitudinal modulus [11]:

$$E_{22} = \frac{E_f E_m}{E_m V_f + E_f V_m}.$$ (1)

Transverse modulus:

$$E_{11} = E_f V_f + E_m V_m.$$ (2)

Major Poisson's ratio:

$$\mu_{12} = \mu_f V_f + \mu_m V_m.$$ (3)

Minor Poisson's ratio:

$$\mu_{21} = \frac{E_{22}}{E_{11}} \mu_{12}.$$ (4)

Shear modulus:

$$G_{12} = \frac{G_f G_m}{G_f V_m + G_m V_f},$$ (5)

where subscripts f and m refers to fibre and matrix respectively.

Continuous fiber angle-ply lamina:

$$\frac{1}{E_{XX}} = \frac{cos^4 \Theta}{E_{12}} + \frac{sin^4 \Theta}{E_{22}} \left[\frac{1}{G_{12}} - \frac{2\mu}{E_{11}} \right] sin^2 \Theta cos^2 \Theta;$$ (6)

$$\frac{1}{E_{yy}} = \frac{sin^4 \Theta}{E_{11}} + \frac{cos^4 \Theta}{E_{22}} \left[\frac{1}{G_{12}} - \frac{2\mu}{E_{11}} \right] sin^2 \Theta cos^2 \Theta;$$ (7)

$$\mu_{xy} = E_{XX} \left[\frac{\mu_{12}}{E_{11}} \left[sin^4 \Theta + cos^4 \Theta \right] \right] - \left[\frac{1}{E_{XX}} + \frac{1}{E_{yy}} - \frac{1}{G_{12}} \right] sin \Theta cos \Theta;$$ (8)

$$\frac{1}{G_{xy}} = 2 \left[\frac{2}{E_{11}} + \frac{2}{E_{22}} + \frac{4\mu_{12}}{E_{11}} - \frac{1}{G_{12}} \right] sin^2 \Theta cos^2 \Theta + \frac{1}{G_{12}} \left[sin^4 \Theta + cos^4 \Theta \right]$$ (9)

For the dome shape part of the rocket motor casing calculating stress is divided into circumferential and axial stresses. Moreover the wall thickness must be calculated. The equations below show all principles.

Circumferential stress [12]:

$$\sigma_c = \frac{pR}{h}.$$ (10)

Axial stress:

$$\sigma_a = \frac{pR}{2h}.$$ (11)

Wall thickness:

$$h = \frac{pR}{\bar{\sigma}},$$ (12)

where R is mandrel radius; Θ is fibre angle and h is dome height.

The stress strain relation of a composite lamina may be written in the following matrix from where the Q_{ij} are defined in terms of lamina. Young's modulus and Poisson's ratio as follows:

$$Q_{11} = \frac{E_{11}}{1 - \mu_{12}\mu_{21}};$$ (13)

$$Q_{22} = \frac{E_{22}}{1 - \mu_{12}\mu_{21}};$$ (14)

$$Q_{12} = \frac{\mu_{12} E_{11}}{1 - \mu_{12}\mu_{21}};$$ (15)

$$Q_{66} = Q_{12};$$ (16)

$$Q_{16} = Q_{26}.$$ (17)

The terms within [Q] are defined to be:

$$\overline{Q}_{11} = Q_{11} cos^4 \Theta + 2(Q_{12} + 2Q_{66}) sin^2 \Theta cos^2 \Theta + Q_{22} sin^4 \Theta;$$ (18)

$$\overline{Q}_{22} = Q_{11} sin^4 \Theta + 2(Q_{12} + 2Q_{66}) sin^2 \Theta cos^2 \Theta + Q_{22} cos^4 \Theta;$$ (19)

$$\overline{Q}_{12} = (Q_{11} + Q_{22} + 2Q_{12}) sin^2 \Theta cos^2 \Theta + Q_{66} (sin^4 \Theta + cos^4 \Theta);$$ (20)

$$\overline{Q}_{66} = (Q_{11} + Q_{22} - 2Q_{12} - 2Q_{66}) sin^2 \Theta cos^2 \Theta + Q_{66} (sin^4 \Theta + cos^4 \Theta);$$ (21)

$$\overline{Q}_{16} = (Q_{11} - Q_{22} - 2Q_{66}) sin \Theta cos^3 \Theta + (Q_{11} - Q_{22} + 2Q_{66}) sin^3 \Theta cos \Theta;$$ (22)

$$\overline{Q}_{26} = (Q_{11} - Q_{22} - 2Q_{66})\sin^3\Theta\cos\Theta +$$
$$+ (Q_{12} - Q_{22} + 2Q_{66})\sin\Theta + \cos^3\Theta. \qquad (23)$$

Combining these relations and arranged in a matrix form as shown in this equation below.

$$\begin{bmatrix} \sigma_x \\ \sigma_y \\ \tau_{xy} \end{bmatrix} = \begin{bmatrix} \overline{Q}_{11} & \overline{Q}_{12} & \overline{Q}_{13} \\ \overline{Q}_{21} & \overline{Q}_{22} & \overline{Q}_{23} \\ \overline{Q}_{31} & \overline{Q}_{32} & \overline{Q}_{33} \end{bmatrix} \begin{bmatrix} \varepsilon_x \\ \varepsilon_y \\ \varepsilon_{xy} \end{bmatrix} + Z_k \begin{bmatrix} \overline{Q}_{11} & \overline{Q}_{12} & \overline{Q}_{13} \\ \overline{Q}_{21} & \overline{Q}_{22} & \overline{Q}_{23} \\ \overline{Q}_{31} & \overline{Q}_{32} & \overline{Q}_{33} \end{bmatrix} \begin{bmatrix} k_x \\ k_y \\ k_{xy} \end{bmatrix}. \qquad (24)$$

The same relationship is expressed in more compact form below:

$$[\sigma]_k = [\overline{Q}]_k[\varepsilon^0] + Z_k[\overline{Q}]_k[k]. \qquad (25)$$

To combine the lamina stiffness it is necessary to invoke the definition of stress and moment resultant, N and M as integral of stress through the thickness of the lamina. The overall stiffness properties of a composite lamina may now be expressed via the following matrix equation. Where the A_{ij}, B_{ij}, D_{ij} are summation of lamina stiffness values, defined as shown:

$$\begin{bmatrix} N_x \\ N_y \\ N_{xy} \end{bmatrix} = \begin{bmatrix} A_{11} & A_{12} & A_{13} \\ A_{21} & BA_{22} & A_{23} \\ A_{31} & A_{32} & A_{33} \end{bmatrix} \begin{bmatrix} \varepsilon_x^0 \\ \varepsilon_y^0 \\ \varepsilon_{xy}^0 \end{bmatrix} + \begin{bmatrix} B_{11} & B_{12} & B_{13} \\ B_{21} & B_{22} & B_{23} \\ B_{31} & B_{32} & B_{33} \end{bmatrix} \begin{bmatrix} k_x \\ k_y \\ k_{xy} \end{bmatrix}; \qquad (26)$$

$$\begin{bmatrix} M_x \\ M_y \\ M_{xy} \end{bmatrix} = \begin{bmatrix} B_{11} & B_{12} & B_{13} \\ B_{21} & B_{22} & B_{23} \\ B_{31} & B_{32} & B_{33} \end{bmatrix} \begin{bmatrix} \varepsilon_x^0 \\ \varepsilon_y^0 \\ \varepsilon_{xy}^0 \end{bmatrix} + \begin{bmatrix} D_{11} & D_{12} & D_{13} \\ D_{21} & D_{22} & D_{23} \\ D_{31} & D_{32} & D_{33} \end{bmatrix} \begin{bmatrix} k_x \\ k_y \\ k_{xy} \end{bmatrix}. \qquad (27)$$

Each component of the [A], [B], [D] matrixes is defined by equations which is shown below:

$$A_{ij} = \sum_{k=1}^{n} (\overline{Q}_{ij})_k (h_k - h_{k-1}); \qquad (28)$$

$$B_{ij} = \frac{1}{2}\sum_{k=1}^{n} (\overline{Q}_{ij})_k (h_k^2 - h_{k-1}^2); \qquad (29)$$

$$D_{ij} = \frac{1}{3}\sum_{k=1}^{n} (\overline{Q}_{ij})_k (h_k^3 - h_{k-1}^3); \qquad (30)$$

$$[A^*] = A^{-1}; \qquad (31)$$

$$[B^*] = [A^{-1}][B]; \qquad (32)$$

$$[C^*] = [B][A^{-1}] = [B^*]^T; \qquad (33)$$

$$[D^*] = [D] - [B][A^{-1}][B]; \qquad (34)$$

$$[A^1] = [A^*] - [B^*][D^{*-1}][C^*] - [A^*] + [B^*][D^{*-1}][B^*]^T; \qquad (35)$$

$$[B^1] = [B^*][D^{*-1}]; \qquad (36)$$

$$[C^1] = [D^{*-1}][C^*] = [B^1]^T = [B^1]; \qquad (37)$$

$$[D^1] = [D^{*-1}]; \qquad (38)$$

$$\begin{bmatrix} \varepsilon \\ \hline k \end{bmatrix} = \begin{bmatrix} A^1 & B^1 \\ B^1 & D^1 \end{bmatrix} \begin{bmatrix} N \\ M \end{bmatrix}. \qquad (39)$$

4. Tsai-Wu criterion

The *Tsai-Wu* criterion is applied to determine the factor of safety for composite orthotropic shells. This criterion considers the total strain energy (both distortion energy and dilatation energy) for predicting failure [13]. It is more general than the *Tsai-Hill* failure criterion because it distinguishes between compressive and tensile failure strengths.

For a 2D state plane stress ($\sigma_3 = 0$, $\tau_{13} = 0$, $\tau_{23} = 0$), the *Tsai-Wu* failure criterion is expressed as:

$$F_1\sigma_1 + F_2\sigma_2 + 2F_{12}\sigma_1\sigma_2 + F_{11}\sigma_1^2 +$$
$$+ F_{22}\sigma_2^2 + F_6\tau_{12} + F_{66}\tau_{12}^2 = 1. \qquad (40)$$

The coefficients of the orthotropic *Tsai-Wu* failure criterion are related to the material strength parameters of the lamina and are determined by experiments. They are calculated from these formulas:

$$F_1 = \left(\frac{1}{X_1^T} - \frac{1}{X_1^C}\right); \qquad (41)$$

$$F_2 = \left(\frac{1}{X_2^T} - \frac{1}{X_2^C}\right); \qquad (42)$$

$$F_{12} = -\frac{1}{2}\sqrt{\frac{1}{X_1^T X_1^C}\frac{1}{X_2^T X_2^C}}; \qquad (43)$$

$$F_{11} = \frac{1}{X_1^T X_1^C}; \qquad (44)$$

$$F_{22} = \frac{1}{X_2^T X_2^C}; \qquad (45)$$

$$F_6 = \left(\frac{1}{X_{12}^T} - \frac{1}{X_{12}^C} \right); \qquad (46)$$

$$F_{66} = \frac{1}{X_{12}^T \cdot X_{12}^C}, \qquad (47)$$

where X_1^T is tensile material strength of laminate along fiber direction; X_1^C is compressive material strength of laminate along fiber direction; X_2^T is tensile material strength of laminate transverse to fiber direction; X_2^C is compressive material strength of laminate transverse to fiber direction; X_{12}^T is positive shear strength of laminate; X_{12}^C is negative shear strength of laminate (the solver considers it equal to

the positive shear strength).

The stress state of the lamina calculated is described by the components: σ_1, σ_2, and τ_{12}, where: σ_1 is laminate stress along fiber direction; σ_2 is laminate stress transverse to fiber direction; τ_{12} is laminate shear stress.

5. Modelling results

After finite element method calculation three characteristics were observed, stresses, deformations and failures [14]. On the failure criteria setup three failure components were employed. Maximum stress, maximum deformation and *Tsai-Wu* failure criteria [15]. Below there are graphs with processed data.
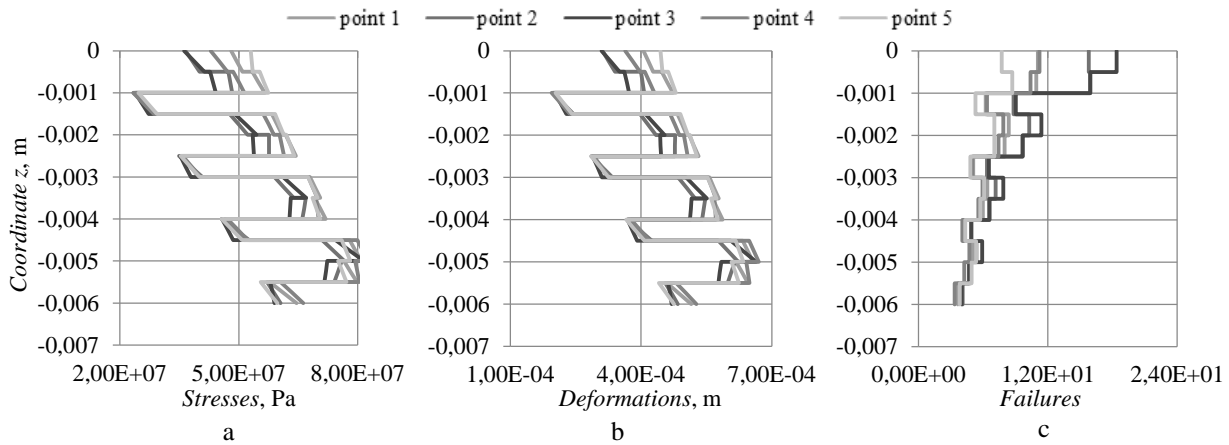

Fig. 5 Nose stresses, deformations and failures. Zone – A, probe point – 6: a – laminate stresses, b – laminate deformations, c – laminate failures

At the dome – nose section A where probe point 6 was sampled it was found that stress values were from $2.47E + 07$ Pa on third composite laminate layer to $7.72E + 07$ Pa on eleventh layer. The deformations were from $2,04E - 04$ m on third layer to $6.70E - 04$ m on tenth layer. The failures were from $3.84E + 00$ on twelfth layer to $1.84E + 01$ on first layer.

At the pipe section B where probe points 3, 4 and 5 were sampled it was found that stress was smallest at point 3 location were values were from $5.65E + 07$ Pa on

the first layer to $1.15E + 08$ Pa on the third layer.

The deformations were from $4.79E - 04$ m on first layer to $9.17E - 04$ m third layer. The failures were form $3.58E + 00$ on twelfth layer to $1.01E + 01$ on third layer.

At the nozzle section C where probe points 1 and 2 were sampled it was found that stress was smallest at point 1 where values were from $3.35E + 06$ Pa on eleventh layer to $1.64E + 07$ Pa on the third layer. On the point 2 location found that stress values were from
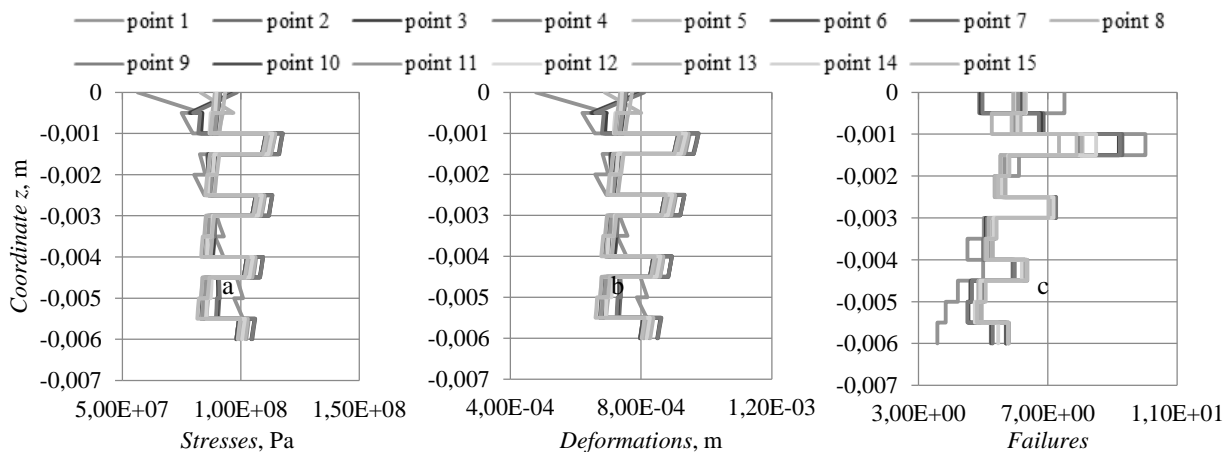

Fig. 6 Body stresses, deformations and failures. Zone – B, probe points – 3, 4, and 5: a – laminate stresses, b – laminate deformations, c – laminate failures
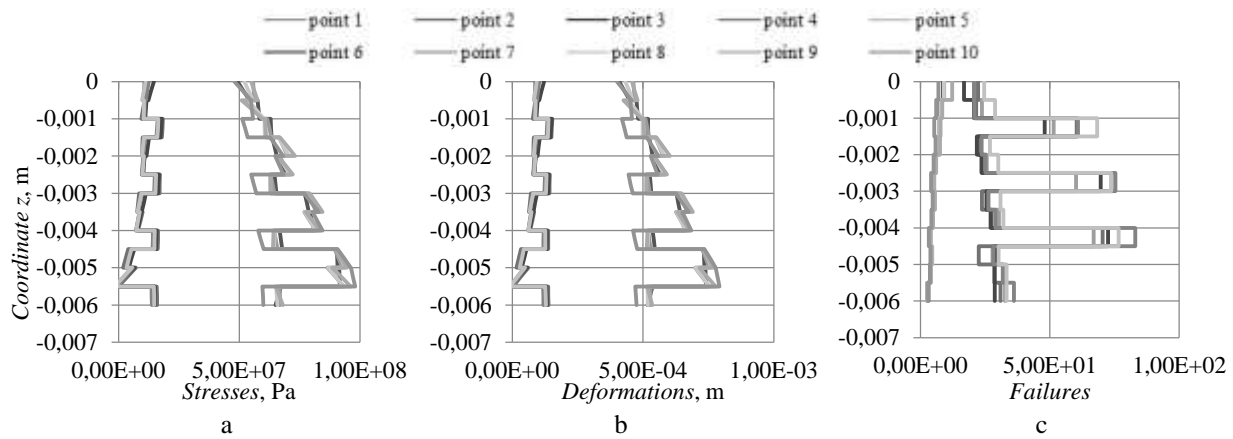
Fig. 7 Nozzle stresses, deformations and failures. Zone – C, probe points – 1 and 2: a – laminate stresses, b – laminate deformations, c – laminate failures

$5.15E + 07$ Pa on first layer to $9.80E + 07$ Pa on eleventh layer. The deformations on the point 1 location were from $-1,01E - 05$ m on eleventh layer to $1.38E - 04$ m on third layer. On the point 2 location found that stress values were from $4.28E - 04$ m on first layer to $7.92E - 04$ m on eleventh layer. The failures on the point 1 location was form $3.00E + 00$ on twelfth layer to $1.23E + 01$ on first layer. On the point 2 location failures were form $3.58E + 00$ on twelfth layer to $1.00E + 01$ on ninth layer.

6. Conclusion

1. In this paper one analyzed geometric model of solid rocket motor casing which is made of composite materials (carbon fiber) strength characteristics when pressure of combustion chamber was 6 MPa. The analyzed model distinguished into main zones. A - dome, B - pipe, C - nozzle. In the particular places of the given zones one measures composite laminate deformations, stresses and failures. The layer thickness of composite material was – 500 μm. Whole casing thickness was – 6 mm. The body is made of 12 layers. The laying pattern of the composite was +45,°-45, 90°.

2. Strength characteristics were measured according to method of finite elements. From data received from finite element method solver software (Ansys composite PrePost), the places loaded most were probed to determine strength of the laminate for the projected pressure. To probe, the incision was made round the axis where 5 sampling elements were taken and compared, and given in the graphs. Altogether 30 sampling elements were determined in the six places of the model.

3. It was found that biggest stresses occurred on the C zone 2 point at the eleventh composite laminate layer where readings showed $9.80E + 07$ Pa. Smallest stresses were found on C zone 1 point at eleventh layer were readings was $3,35E + 06$ Pa. The biggest deformations were found on the B zone 3 point at third layer were values was $9.17E - 04$ m. Smallest deformations were found on C zone 1 point eleventh layer where readings were $-1.01E - 05$ m. Highest possibility of laminate failure was found on C zone 1 point second layer was $3.00E + 00$. Lowest possibility of delamination was found on the dome A section 6 point at first layer where sampling element values $1.84E + 01$.

References

1. National Aeronautics and Space Administration (NASA). 2012. Academy of Aerospace Quality. Available: http://aaq.auburn.edu/. Last accessed 2014 Feb 24.
2. Space Technology Mission Directorate. 2013. Composite Cryotank Technologies and Demonstration (CCTD). [ONLINE] Available at: http://gcd.larc.nasa.gov/wp-content/uploads/2013/07/FS_CCTD_factsheet.pdf. [Last Accessed 2014 May 04].
3. **Vasiliev, V. Valery.** 2009. Composite Pressure Vessels: Design, Analysis, and Manufacturing. Blacksburg, Vir. : Bull Ridge Pub. 690p.
4. **Xia, M.; Takayanagi, M.; Takayanagi**, H. 2001. Analysis of filament-wound fiber-reinforced sandwich pipe under combined internal pressure and thermo mechanical loading, Compos Struct,: 273-283. http://dx.doi.org/10.1016/S0263-8223(00)00137-9.
5. **Lee, S.Y.; Springer, G.S.** 1990. Filament winding cylinder—part III: Selection of the process variables, Journal of Composite Materials, 24(12): 1344-1366. http://dx.doi.org/10.1177/002199839002401204.
6. **Moeykens, S.** 2014. World-Class Composites Analysis by Alinghi. [ONLINE] Available at: http://www.ansys.com/staticassets/ANSYS/staticassets/resourcelibrary/article/AA-V4-I1-World-Class-Composites-Analysis-by-Alinghi.pdf. [Last Accessed 2014 May 02].
7. **Kaw, Autar K.** 2006. Polymer matrix composites. In: Taylor & Francis Group (ed), Mechanics of composite materials. 2nd ed. Boca Raton: Taylor & Francis, 25-29.
8. **Toyo Tanso.** 2014. Special graphite (Isotropic graphite). [ONLINE] Available at: http://www.toyotanso.co.jp/Products/Special_graphite/data_en.html. [Last Accessed 2014 May 04].
9. **McLaughlan, B.; Forth, Scott C.; Grimes-Ledesma, Lorie R.** 2011. Composite Overwrapped Pressure Vessels, a primer. NASA/SP–2011–573. 30p.
10. **Krikanov, A. Alexis**, 2000. Composite pressure vessels with higher stiffness. Composite Structures 48: 119-127. http://dx.doi.org/10.1016/S0263-8223(99)00083-5.

11. **Parnas, L.; Katirci, N.** 2002. Design of fiber-reinforced composite pressure vessels under various loading conditions. Composite Structures 58: 83-95. http://dx.doi.org/10.1016/S0263-8223(02)00037-5.

12. **Rao Yarrapragada, K.S.S.; Krishna Mohan, R.; Kiran, B.Vijay.** 2012. Composite Pressure Vessels. International Journal of Research in Engineering and Technology1(4): 597-618.

13. **Tsai, S.W.; Wu, E.M.** 1971. A general theory of strength for anisotropic materials, J Compos Mater, 5: 58-80. http://dx.doi.org/10.1177/002199837100500106

14. **ANSYS** (2014). Structural Technology Tips - Composites. [ONLINE] Available at: http://ansys.com/Products/Simulation+Technology/Structural+Analysis/Structural+Technology+Leadership/Technology+Tips/Simulation+of+3-D+Composites. [Last Accessed 2014 May 02].

15. **Krikanov, A.A.; Soni, S.R.** 1995. Minimum weight design of pressure vessel with constraints on stiffness and strength. In: Proceedings of the 10th ASC Technical Conference on Composite Materials, Santa Monica, CA,: 107±13.

A. Fedaravičius, S. Račkauskas, E. Sližys, A. Survila

KIETO KURO RAKETINIO VARIKLIO KOMPOZITINIO KORPUSO ATSPARUMINIŲ CHARAKTERISTIKŲ TYRIMAS

R e z i u m ė

Straipsnyje pateiktas Kauno technologijos universiteto Gynybos technologijų instituto mokslininkų sukurtas kieto kuro raketinis variklis. Konstrukcijos masei bei sujungimo detalių kiekiui sumažinti pasiūlyta naudoti kompozitines medžiagas – anglies pluoštą. Naudota juostos vyniojimo apie ašį metodika. Nustatytas reikiamas sluoksnių skaičius bei vyniojimo kampas. Šiuo atveju naudotas 45°, -45°, 90° vyniojimo raštas, kuris leidžia maksimaliai išlaikyti reikiamą konstrukciją nuo galimų trūkių variklio veikimo metu. Šilumos izoliacijai naudotas "tanso" grafitas, kuris modeliuotas kaip atskiras komponentas nepriklausantis nuo kompozito modelio, bet buvo naudotas bendros sistemos modelyje.

A. Fedaravičius, S. Račkauskas, E. Sližys, A. Survila

INVESTIGATION OF SOLID ROCKET STRENGHT CHARACTERISTICS BY EMPLOYING COMPOSITE MATERIALS

S u m m a r y

This paper presents the investigation of solid rocket motor by scientists of Kaunas University of technology Institute of defence technologies. Because of the mass and assembly complexity one proposes to use composite materials (carbon fiber) for motor case manufacturing. Filament winding method was implemented. For best composite performance determined optimal thickness of laminate and winding angles. For this application one uses 45°, -45°, 90° winding angle patterns, witch let exploit the composite for maximum performance from probable composite fractures. For the thermal protection one uses "tanso" graphite to shield motor nozzle from composite delamination caused by high pressure, temperature and corrosion. Thermal shielding was modelled independently from composite model but used in the final model.